Hindawi
Advances in Civil Engineering
Volume 2019, Article ID 5824972, 11 pages
https://doi.org/10.1155/2019/5824972

Research Article

Lever-Type Tuned Mass Damper for Alleviating Dynamic Responses

Eun-Taik Lee[1] and Hee-Chang Eun[2]

[1]*Department of Architectural Engineering, Chung-Ang University, Seoul, Republic of Korea*
[2]*Department of Architectural Engineering, Kangwon National University, Chuncheon, Republic of Korea*

Correspondence should be addressed to Hee-Chang Eun; heechang@kangwon.ac.kr

Received 9 June 2019; Revised 25 September 2019; Accepted 1 October 2019; Published 31 October 2019

Academic Editor: Rafael J. Bergillos

This study considers the structural vibration control by a lever-type tuned mass damper (LTMD). The LTMD has a constraint condition to restrict the motion at both ends of the lever. The LTMD controls the dynamic responses at two locations combining the tuned mass damper (TMD) and the constraint condition. The parameters of the LTMD are firstly estimated from the TMD parameters and should be modified by them to obtain from numerical results. The effectiveness of the LTMD is illustrated in two numerical experiments, and the sensitivity of the parameters is numerically investigated. It is shown that the LTMD leads to the remarkable displacement reduction and exhibits more definite control than the TMD system because the LTMD controls the vibration responses at two DOFs. More displacement responses are reduced when the installation locations of the LTMD coincide with the nodes to represent the largest modes' values at the first and second modes. The application of the LTMD at the dynamic system of a few degrees of freedom (DOFs) is more effective than the system of many DOFs.

1. Introduction

Many countries specify the seismic-resistant design to protect the building structures and the residents inside due to earthquakes. Bracing and shear wall must be seismic-resistant members to reduce the structural responses by improving the lateral stiffness of a structure. The existing methods to improve the seismic performance of structures consist of controlling the plastic hinge occurrence, increasing the deformation capacity and dissipated energy, strengthening or changing the structural system, and enhancing the lateral stiffness.

The dynamic control systems can be considered for more definite vibration control. The utilization of a seismic control system to dissipate earthquake energy has been raised to reduce loss of lives and property caused by seismic disasters. The dynamic control systems are divided into three different systems of passive, active, and hybrid controls.

A tuned mass damper (TMD) is a kind of passive control system installed on a structure for reducing the dynamic responses. The frequency of the TMD is tuned to the structural frequency, and the energy is dissipated. The Citigroup Center in New York City, Chiba Port Tower in Japan, John Hancock Tower in Boston, Canadian National Tower in Toronto, Crystal Tower in Japan, Taipei 101 in Taiwan, etc., are representative examples to install TMDs. The design theory for the TMD was initiated by Ormondroyd and Den Hartog [1] in 1928. Various theories have been developed for the designs of undamped and damped TMD installed on the undamped and damped single-degree-of-freedom (SDOF) system subjected to harmonic excitation or seismic excitation.

Tsai and Lin [2] proposed the optimum tuning frequency and damping ratio of the TMD through a sequence of curve-fitting schemes. Abdulsalam et al. [3] suggested the optimum frequency ratio and damping ratio of the TMD installed on a structure subjected to an earthquake loading. Den Hartog [4] did not consider the damping effect of the primary structure. Abubakar and Farid [5] presented the optimum design parameters for the TMD considering the damping of

the primary structure. Okhovat et al. [6] performed a parametric study to evaluate the effectiveness for the TMD at Tehran Tower through the finite element analysis. Murudi and Mane [7] investigated the seismic effectiveness of TMD and found that the TMD is not affected by the intensity of ground motion. Warburton and Ayorinde [8] studied the effect on the optimum parameter conditions of light damping in the primary system. Farghaly and Ahmed [9] discussed the design procedure and the applications through a case study of a symmetrical moment resistance frame twenty-story three-dimensional model. Nigdeli and Bekdas [10] investigated the control effect depending on the location of a TMD on a seismic structure for an effective response reduction. Bakre and Jangid [11] derived the optimum parameters of TMD installed on a viscously damped SDOF system for various combinations of excitation and response parameters.

The strategies to improve seismic performance may be established by the structural type and assessment results. Stoica [12] provided a seismic retrofitting method to consolidate conventional methods and seismic device such as TMD. Brendike and Petryna [13] studied the TMD to control the dynamic responses as a seismic retrofit device of RC frame structures. Suzuki et al. [14] developed a seismic control device to increase damping of an old bridge for seismic retrofit. Nawrotzki et al. [15] introduced the effectiveness of the tuned mass control systems for the seismic retrofitting of existing structures.

This study considers the effectiveness of LTMD installed between the two nodes in the structure. The LTMD controls the structural responses and is designed using a constraint condition of the lever responses as well as the optimum parameters of the TMD. This work performs the numerical study according to the design parameters of the LTMD and compares the seismic effect by the LTMD and TMD in the numerical experiment. It is shown that the LTMD is more effective in controlling the dynamic responses than the TMD. More displacement responses are reduced when the installation locations of the LTMD coincide with the nodes to represent the largest modes values at the first and second modes. It is shown that the application of the LTMD at the dynamic system of a few DOFs is more effective than the system of many DOFs.

2. Formulation

2.1. TMD Design Parameters. A primary structure described by n DOFs can be idealized as a SDOF structure. Figure 1 represents a SDOF system consisting of a primary structure and a TMD. Many researchers provided the optimum parameter values of the TMD for reducing the responses of the undamped or damped system subjected to harmonic forces or earthquake load.

The dynamic equation of motion for the systems can be written by

$$\begin{bmatrix} m_p & 0 \\ 0 & m_T \end{bmatrix} \begin{bmatrix} \ddot{u}_p \\ \ddot{u}_T \end{bmatrix} + \begin{bmatrix} c_p + c_T & -c_T \\ -c_T & c_T \end{bmatrix} \begin{bmatrix} \dot{u}_p \\ \dot{u}_T \end{bmatrix} + \begin{bmatrix} k_p + k_T & -k_T \\ -k_T & k_T \end{bmatrix} \begin{bmatrix} u_p \\ u_T \end{bmatrix} = \begin{bmatrix} F_p \\ F_T \end{bmatrix}, \quad (1)$$

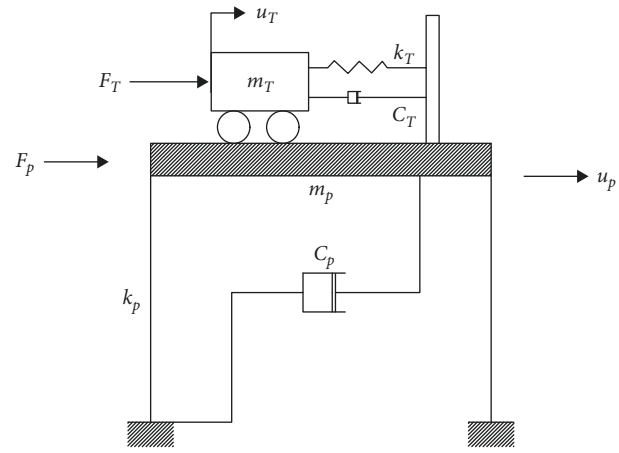

Figure 1: A TMD installed on a SDOF primary structure.

where the subscripts "p" and "T" indicate the primary structure and the TMD, respectively, m, c, and k denote the mass, damping, and stiffness, respectively, and u and F are the displacement response and external force, respectively.

The optimum design parameters for the TMD take different forms depending on the types of external forces and the presence of the damping in the primary structure. Considering the harmonic forces and the earthquake load as the external forces, $F_p = F_0 e^{i\Omega t}$ and $F_T = 0$ and $F_p = -m_p \ddot{u}_g$ and $F_T = -m_T \ddot{u}_g$, respectively. F_0 and $\ddot{u}_g$ represent the force magnitude and the acceleration of earthquake, respectively.

Tables 1 and 2 denote the optimum parameters suggested by various researchers according to the undamped and damped primary structures, respectively. In the tables,

$\mu = m_T/m_p$: mass ratio

$\xi_p = c_p/2\omega_p m_p$: damping ratio of the primary structure

$\xi_T = c_T/2\omega_T m_T$: damping ratio of the TMD

$\omega_p = \sqrt{k_p/m_p}$: natural frequency of the primary structure

$\omega_T = \sqrt{k_T/m_T}$: natural frequency of the TMD

$f = \omega_T/\omega_p$: natural frequency ratio

f^{OPT}: optimal frequency ratio

ξ_T^{OPT}: optimal damping ratio of the TMD

It is observed that the optimal parameters in Tables 1 and 2 are deeply affected by the mass ratio between the primary structure and TMD and the damping ratio of the primary structure. However, the numerical values of the parameters are very close despite the different mathematical forms. From the parameters of the TMD, the LTMD parameters can be designed, and their effectiveness is investigated.

2.2. LTMD. This section considers the parameter design of a LTMD based on the concept of the TMD. The LTMD shown in Figure 2 is installed between the adjacent two nodes in a structure; it is designed by modifying the TMD design parameters and controls the dynamic responses at the two nodes unlike the TMD. The LTMD consists of the massless lever, the masses, springs, and dampers at both ends, and the

Table 1: Optimal TMD parameters for undamped primary structures.

Loading/researchers	f^{OPT}	ξ_T^{OPT}
H.F./Den Hartog [1]	$1/(1+\mu)$	$\sqrt{(3/8)(\mu/(1+\mu))}$
H.A./Warburton [16]	$(1/(1+\mu))\sqrt{(2-\mu)/2}$	$\sqrt{3\mu/(4(1+\mu)(2-\mu))}$
W.N.F./Warburton [16]	$(1/(1+\mu))\sqrt{(2+\mu)/2}$	$\sqrt{(\mu(4+3\mu))/(8(1+\mu)(2+\mu))}$
W.N.A./Warburton [16]	$(1/(1+\mu))\sqrt{(2-\mu)/2}$	$\sqrt{(\mu(4-\mu))/(8(1+\mu)(2-\mu))}$

H.F., harmonic force; H.A., harmonic accelerations; W.N.F., white noise force; W.N.A., white noise accelerations.

Table 2: Optimal TMD parameters for damped primary structures.

Loading/researchers	f^{OPT}	ξ_T^{OPT}
H.F./Abubakar [5]	$(1/(1+\mu))(1-1.5906\xi_p\sqrt{\mu/(1+\mu)})$	$\sqrt{(3/8)(\mu/(1+\mu))}+0.1616\xi_p/(1+\mu)$
Sadek [17]	$(1/(1+\mu))(1-\xi_p\sqrt{(\mu/(1+\mu))})$	$(\xi_p/(1+\mu))+\sqrt{\mu/(1+\mu)}$

hinge to restrict the responses at both ends. The system is subjected to a constraint to restrict the interstory drift and provides the control forces at both ends of the lever. The control forces indicate the constraint forces required for satisfying the constraint condition.

The dynamic equation for the LTMD can be written by

$$\begin{bmatrix} m_{T1} & 0 \\ 0 & m_{T2} \end{bmatrix}\begin{bmatrix} \ddot{u}_{T1} \\ \ddot{u}_{T2} \end{bmatrix}+\begin{bmatrix} c_{T1} & 0 \\ 0 & c_{T2} \end{bmatrix}\begin{bmatrix} \dot{u}_{T1} \\ \dot{u}_{T2} \end{bmatrix} +\begin{bmatrix} k_{T1} & 0 \\ 0 & k_{T2} \end{bmatrix}\begin{bmatrix} u_{T1} \\ u_{T2} \end{bmatrix}=\begin{bmatrix} F_{T1} \\ F_{T2} \end{bmatrix}, \tag{2a}$$

$$\text{or } \mathbf{M}_T\ddot{\mathbf{u}}_T+\mathbf{C}_T\dot{\mathbf{u}}_T+\mathbf{K}_T\mathbf{u}_T=\mathbf{F}, \tag{2b}$$

where the subscripts "$T1$" and "$T2$" denote the DOFs at the both ends of the lever, respectively, and the corresponding displacement response and external force are represented by u and F. The system constrained by one constraint condition becomes a SDOF system.

The constraint condition from the relationship of $l_a\theta = u_{T1}$ and $l_b\theta = u_{T2}$ can be written by

$$\alpha u_{T1}=u_{T2}, \tag{3}$$

where $\alpha = l_b/l_a$ and θ denotes the rotational angle at the hinge of the lever.

The dynamic equation of motion for the constrained system was proposed by Udwadia and Kalaba [18] in 1992. The equation was derived by minimizing the Gaussian function as a function by the difference between the constrained and unconstrained accelerations. The dynamic equation for the LTMD system can be expressed by

$$\ddot{\mathbf{u}}_c=\ddot{\mathbf{u}}_a+\mathbf{M}_T^{-1/2}\left(\mathbf{A}\mathbf{M}_T^{-1/2}\right)^{+}(\mathbf{b}-\mathbf{A}\ddot{\mathbf{u}}_a), \tag{4}$$

where $\ddot{\mathbf{u}}_a=-\mathbf{M}_T^{-1}(\mathbf{C}_T\dot{\mathbf{u}}_T+\mathbf{K}_T\mathbf{u}_T-\mathbf{F})$, $\ddot{\mathbf{u}}_c$ and $\ddot{\mathbf{u}}_a$ denote the acceleration vector for the constrained and unconstrained dynamic system, respectively, and the matrix $\mathbf{A}$ and the vector $\mathbf{b}$ represent the coefficients in differentiating equation (3) twice with respect to the time as

$$\mathbf{A}=\begin{bmatrix} \alpha & -1 \end{bmatrix},\quad \mathbf{b}=0. \tag{5}$$

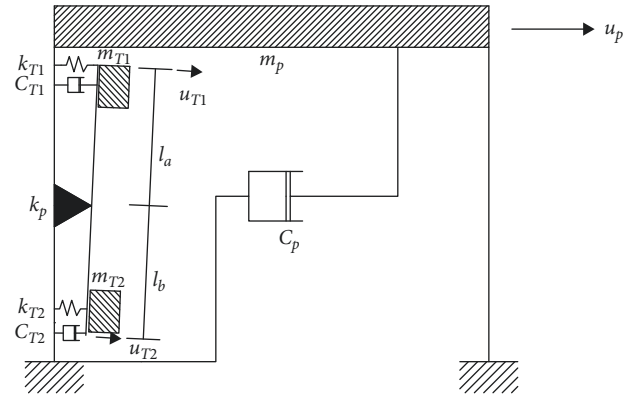

Figure 2: LTMD configuration.

Substituting equations (2a), (2b), and (5) into equation (4), utilizing the linear algebra, and arranging the result, the dynamic equation at the upper DOF of the lever yields

$$m_{T1}\ddot{u}_{T1,c}+c_{T1}\dot{u}_{T1,c}+k_{T1}u_{T1,c}=F_{T1,c}, \tag{6}$$

where $c_{T1}=c_T(\alpha^2m_{T1}^{-1}+m_{T2}^{-1})/(m_{T2}^{-1}+\alpha^2\gamma m_{T2}^{-1})$, $c_{T2}=\gamma c_{T1}$, $k_{T1}=k_T(\alpha^2m_{T1}^{-1}+m_{T2}^{-1})/(m_{T2}^{-1}+\alpha^2\beta m_{T2}^{-1})$, $k_{T2}=\beta k_{T1}$, and $F_{T1,c}=m_{T2}^{-1}(F_{T1}+\alpha F_{T2})/(m_{T2}^{-1}+\alpha^2m_{T1}^{-1})$, $m_{T2}=\eta m_{T1}$.

The coefficients β, γ, and η denote the stiffness ratio, damping ratio, and mass ratio at the one end with respect to the stiffness, damping, and mass at the other end of the lever, respectively.

The dynamic equation at the other end of the lever can be derived by inserting the relation of equation (3) into equation (6). The control forces exerted by the LTMD act on the structure and are obtained by multiplying the second term in the right-hand side of equation (4) by the mass matrix $\mathbf{M}$:

$$\mathbf{F}^c=\mathbf{M}^{1/2}\left(\mathbf{A}\mathbf{M}^{-1/2}\right)^{+}(\mathbf{b}-\mathbf{A}\ddot{\mathbf{u}}_a). \tag{7}$$

The dynamic responses of the LTMD are controlled by the control forces estimated by equation (7), and the forces affect the responses of the entire structure.

The LTMD is designed by the flowchart shown in Figure 3. It is shown that the TMD parameters are firstly estimated using assumed mass ratio μ and Tables 1 and 2. The design parameters of the LTMD α, β, γ, and η are selected by

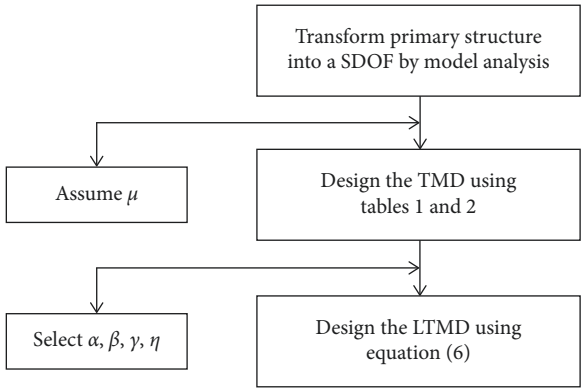

Figure 3: Flowchart for designing the LTMD.

the numerical values minimizing the dynamic responses of the structure subjected to external excitations. In the design process, the optimum values of the variables μ, α, β, γ, and η are estimated numerically. The effectiveness and superiority of the LTMD are numerically illustrated in the following two examples.

3. Applications

3.1. Control of a Three-Story Building Structure. Consider the design of the LTMD installed between the second and third floors in a three-story building structure, as shown in Figure 4, and its dynamic control. The TMD is installed on the floor of the structure to exhibit the largest mode value in the first mode. If we add another TMD for more displacement control, it should be installed at the location to exhibit the highest mode value in the second mode. Utilizing the concept of MTMD (multi-TMD), the LTMD is located at the third and second floor corresponding to the highest mode values in the first and second mode, respectively.

The parameters interdependently affect the dynamic responses and control. The control by the LTMD is numerically evaluated by the design parameters and compared with the dynamic control by the TMD. The mechanical properties of the primary structure are assumed as $m_1 = m_2 = m_3 = 10\,\text{kg}$, $c_1 = c_2 = c_3 = 2\,\text{N·sec/m}$, and $k_1 = k_2 = k_3 = 1,000\,\text{N/m}$.

The primary structure is transformed to a SDOF system using the first natural frequency ω_1 and the corresponding mode shape $\boldsymbol{\varphi}_1$:

$$\begin{aligned} \omega_1 &= 4.45\,\text{rad./sec.}, \\ \boldsymbol{\varphi}_1 &= \begin{bmatrix} 0.445 & 0.8019 & 1.000 \end{bmatrix}^T. \end{aligned} \tag{8}$$

The modal mass can be calculated by

$$\boldsymbol{\varphi}_1^T \mathbf{M} \boldsymbol{\varphi}_1 = 18.4\,\text{kg}. \tag{9}$$

Utilizing the above modal and the optimal parameters presented by Den Hartog and various researchers in Table 1, the optimum parameters of the TMD, f^{OPT} and ξ_T^{OPT}, are calculated using the prescribed mass ratio μ. The TMD parameters are designed selecting the mass ratios of 0.02 and 0.03 for this study.

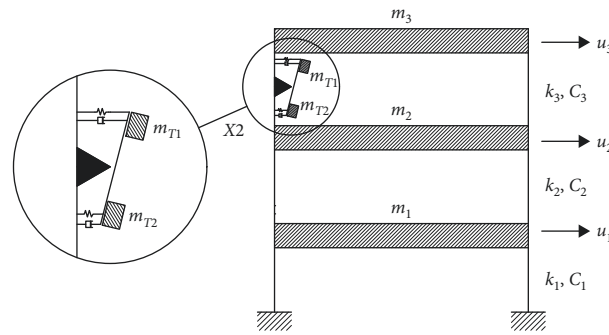

Figure 4: A three-story building structure.

The design parameters α, β, γ, and η of the LTMD may be estimated by the TMD optimum parameters and numerical analysis. This study numerically investigates the dynamic control and design values of those parameters. Firstly, assuming numerical values of α and η with the prescribed mass ratio, the other parameters β and γ to minimize the square root of the sum of the squares (SRSS) by the dynamic responses during an external excitation are determined. And another SRSS is calculated using the predetermined parameters β and γ, and the parameters α and η to minimize the SRSS are also selected. We assume that the half-scaled N-S acceleration components of the 1940 El Centro earthquake acted on the structure during the first 30 seconds. Figure 5(a) represents the N-S acceleration component of the El Centro earthquake.

Figure 5(b) represents the SRSS responses according to the parameters β and γ in substituting the assumed values of $\mu = 0.02$, $\alpha = 0.8091$, and $\eta = 1.0$ into equation (6). The SRSS responses are calculated in the range of $0.7 \le \beta \le 1.15$ and $0.7 \le \gamma \le 1.15$ with the step of 0.05. The minimum values of the SRSS responses are taken at $\beta = 0.75$ and $\gamma = 0.70$. Substituting these values into equation (6) and numerically integrating the second-order differential equation, the SRSS responses are determined according to the parameters α and η and are plotted in Figure 5(c). They exhibit the minimized values at $\alpha = 0.7$ and $\eta = 0.95$. It is observed from the SRSS plots that the design parameters for the LTMD interdependently affect the dynamic responses of the structure.

Figures 5(d)–5(f) compare three dynamic responses of the structure without any dynamic control system, with TMD or LTMD. It is shown that the control system remarkably reduces the dynamic responses. And the LTMD system is more effective in controlling the dynamic responses than the TMD. It is due to the control of the dynamic responses of adjacent two floors unlike the TMD. The control forces or constraint forces necessary to satisfy the constraint condition of the lever act on the structure, and the dynamic responses are controlled by the forces. Figure 5(g) represents the forces acting on the upper mass of the lever, and the forces αF_{T1}^c act on the lower mass. The dynamic control is accomplished by those forces.

Similar process is performed using the mass ratio of $\mu = 0.03$, and Figure 6 shows the numerical results. The minimum SRSS responses in Figures 6(a) and 6(b) appear at the parameters of $\alpha = 1.15$, $\beta = 1.15$, $\gamma = 1.15$, and $\eta = 1.0$. It

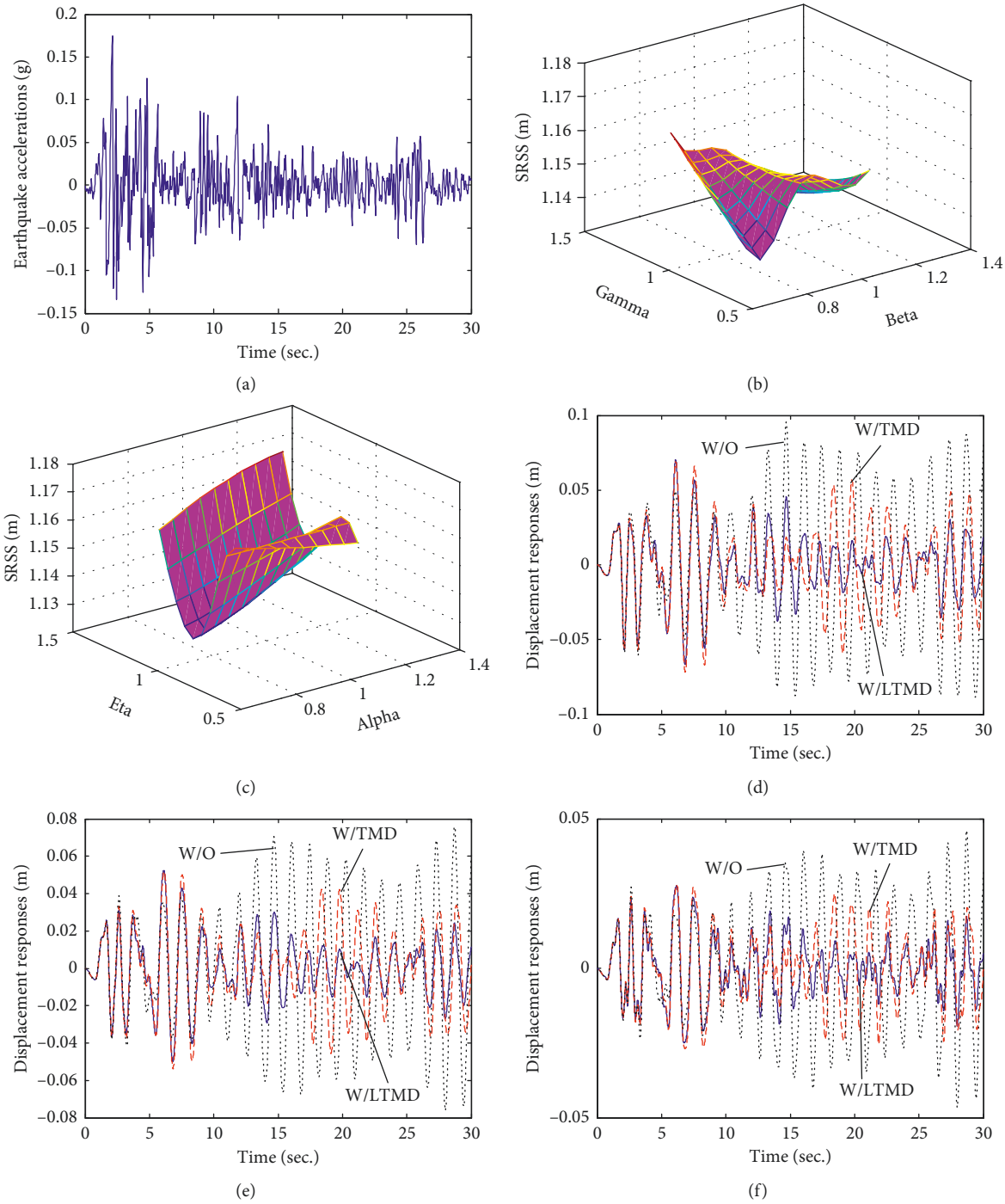

Figure 5: Continued.

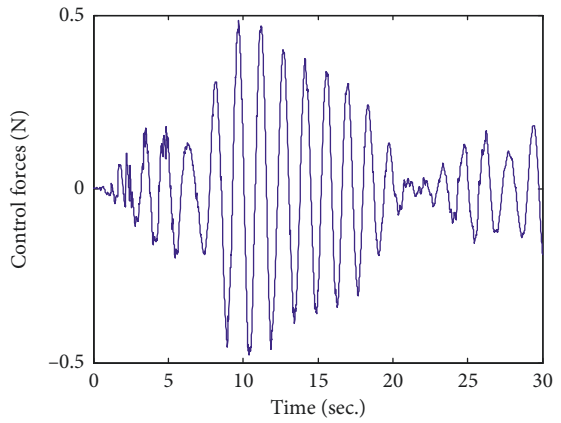

(g)

Figure 5: Numerical results of dynamic responses using the mass ratio $\mu = 0.02$. (a) Earthquake accelerations; (b) SRSS according to β and γ at fixed values of $\alpha = 0.8093$ and $\eta = 1.0$; (c) SRSS according to α and η at fixed values of $\beta = 1.15$ and $\gamma = 1.15$; (d) dynamic responses (3^{rd} floor) at $\alpha = 1.15$, $\beta = 1.15$, $\gamma = 1.15$, and $\eta = 1.0$; (e) dynamic responses (2^{nd} floor); (f) dynamic responses (1st floor); (g) control forces at the upper mass of the lever.

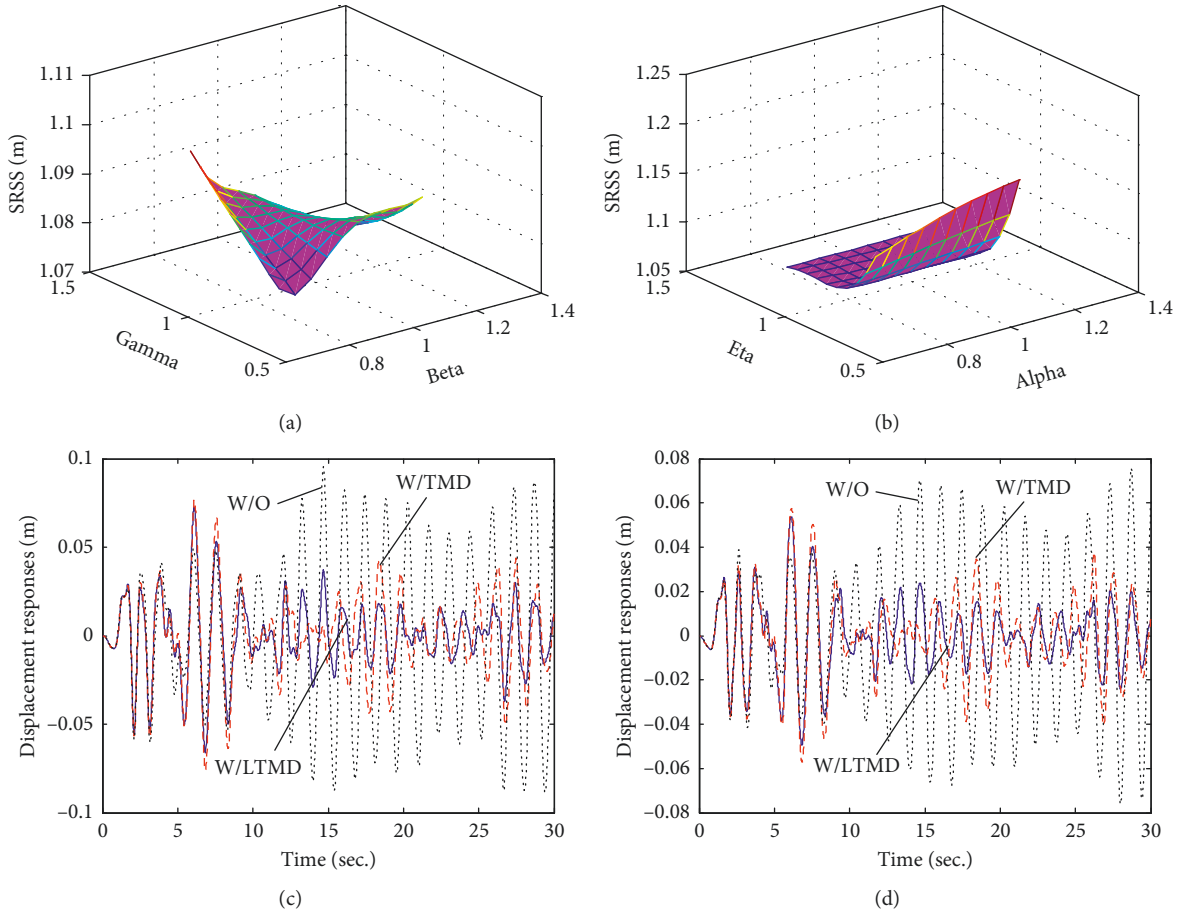

Figure 6: Continued.

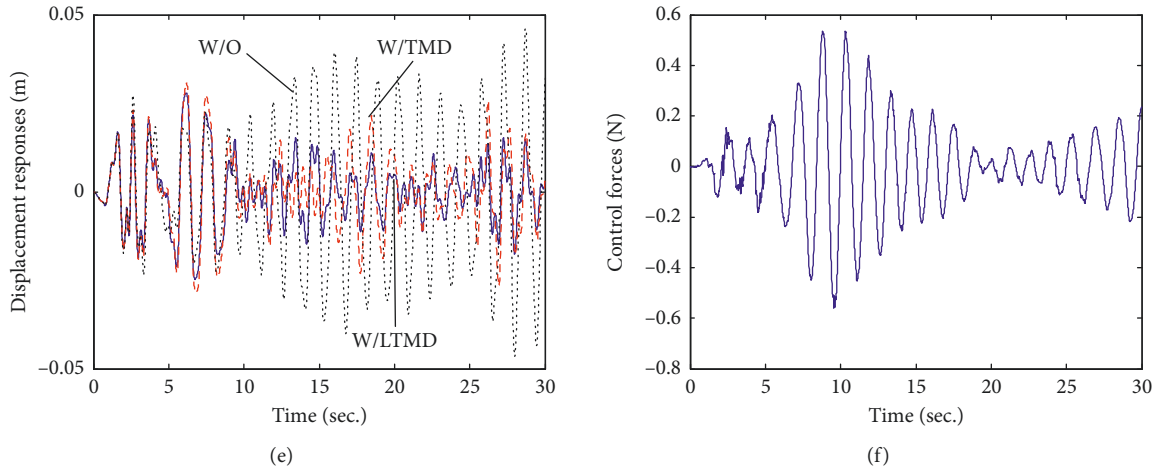

FIGURE 6: Numerical results of dynamic responses using the mass ratio $\mu = 0.03$. (a) SRSS according to β and γ at fixed values of $\alpha = 0.8093$ and $\eta = 1.0$; (b) SRSS according to α and η at fixed values of $\beta = 0.75$ and $\gamma = 0.7$; (c) dynamic responses (3^{rd} floor) at $\alpha = 0.7$, $\beta = 0.75$, $\gamma = 0.7$, and $\eta = 0.95$; (d) dynamic responses (2^{nd} floor); (e) dynamic responses (1st floor); (f) control forces at the upper mass of the lever.

indicates that the LTMD to be installed between two floors corresponding to the highest mode values of the first and second modes is effective in reducing the dynamic responses. It more definitely controls the dynamic responses than the TMD system as shown in Figures 6(c)–6(e). And the LTMD is very effective in reducing the story drift by the control forces as shown in Figure 6(f).

Figure 7 compares the dynamic responses and the control forces in utilizing the coefficient values to minimize the SRSS shown in Figure 5 ($\mu = 0.02$) and Figure 6 ($\mu = 0.03$). It is shown that the dynamic responses are reduced with the increase in the mass ratio. The increase in the mass ratio also leads to the increase in the control forces as shown in Figure 7(c). Though the optimum parameters of the LTMD cannot be explicitly established, it is shown that they can be obtained by numerical experiments and the LTMD system can more definitely control the dynamic responses than the TMD system.

3.2. Control of a Simply Supported Beam. The distance between the locations to represent the largest mode values at the first and second modes increases with the increase in the number of DOFs. In the case of a fixed-end beam shown in Figure 8, one end of the lever should be installed at the midspan to represent the largest mode value at the first mode. This example investigates the vibration control according to the location of the other end of the LTMD and compares the effectiveness with the TMD system.

Assume that the external excitations of 10% magnitude of the earthquake accelerations in Figure 5(a) vertically act at both ends of the beam. The dynamic responses for the first 30 seconds are calculated by integrating the second-order differential equation with the time step of 0.02 seconds. The nodal points and the elements are numbered as shown in figure. A beam with a length of 1 m is modeled using 20 beam elements. The beam has an elastic modulus of 1.95×10^5 MPa and a unit mass of $7,860\ \text{kg/m}^3$. The beam's gross cross section is $b \times h = 75\ \text{mm} \times 9\ \text{mm}$. The damping matrix is assumed as a Rayleigh damping to be expressed by the stiffness and mass matrices with proportionality constants of 0.001 and 0.002, respectively.

In this example, we consider two cases depending on the installation location of the other end of the LTMD: (a) case 1 to position at the node 15 to represent the highest mode value in the second mode and (b) case 2 to position at the node 13 adjacent to the nodes 10 and 15. The sensitivity of the design parameters of the LTMD is numerically investigated. Figure 9(a) represents the SRSS plot of case 1 according to the variation of the parameters β and γ at fixed values of $\mu = 0.03$, $\alpha = 1.414$, and $\eta = 1.0$. The SRSS using the displacement responses at all 19 nodes is calculated with the increase of 0.05 in the ranges of $0.7 \le \beta \le 1.15$ and $0.7 \le \gamma \le 1.15$. It is shown that the minimum SRSS is located at $\beta = 1.15$ and $\gamma = 0.95$. In next stage, the SRSS of the displacements is determined with the increase of 0.05 in the ranges of $0.7 \le \alpha \le 1.15$ and $0.7 \le \eta \le 1.15$ at the fixed parameter values of $\beta = 1.15$ and $\gamma = 0.95$. The optimum values of the parameters in these ranges can be estimated by $\alpha = 1.15$ and $\eta = 0.85$. It is shown in Figure 9(b) that the vibration can be more explicitly controlled with the increase in the parameters α and β in the given ranges rather than the parameters γ and η. It indicates that the vibration is more sensitive to the length ratio of the lever and the stiffness ratio at both ends of the lever.

The SRSS of the displacements is shown in Figures 9(c) and 9(d) when the lever is installed at nodes 10 and 13. Minimum SRSS is obtained when the values of parameters are as follows: $\alpha = 1.15$, $\beta = 1.15$, $\gamma = 0.9$, and $\eta = 0.8$. These plots also show that the length ratio and the stiffness ratio are sensitive to the vibration control of the beam.

Figure 10 compares the displacement responses at nodes 10 and 15 of case 1. The parameter values of $\mu = 0.03$, $\alpha = 1.15$, $\beta = 1.15$, $\gamma = 0.95$, and $\eta = 0.85$ are utilized. It is observed in Figures 10(a) and 10(b) that the dynamic responses are remarkably reduced by the TMD or LTMD. And

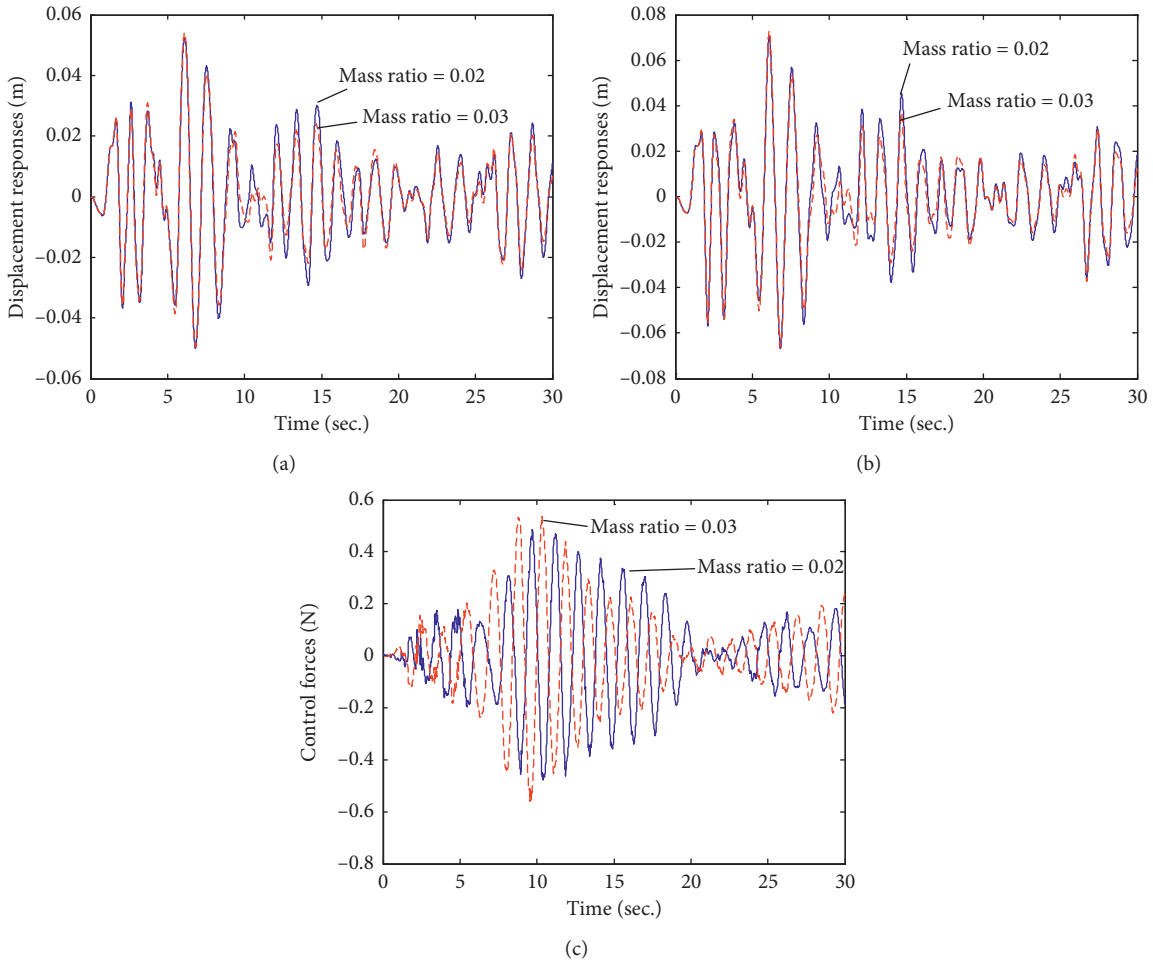

Figure 7: Displacement responses and control forces depending on the mass ratio μ. (a) Dynamic responses (2^{nd} floor); (b) dynamic responses (3rd floor); (c) control forces at the upper mass of the lever.

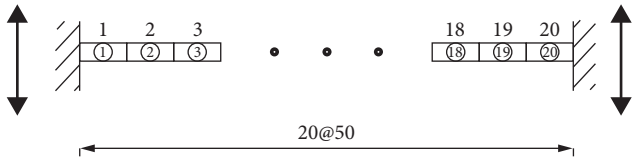

Figure 8: A fixed-ended beam model.

it is found in those plots that the LTMD system can reduce a little more dynamic responses than the TMD system because the LTMD makes an additional control at another node 15 unlike the TMD. Thus, it is shown in Figure 10(c) that the displacement difference between nodes 10 and 15 can be reduced owing to the control force in the satisfaction of the constraint condition of the lever motion.

Figure 11 compares the displacement responses at nodes 10 and 15 depending on the installation locations of the LTMD of two cases. The response difference at two cases cannot explicitly be recognized but the LTMD of case 1 is a little more effective than that of case 2. It is shown that the LTMD is a little more effective when it is installed at the location of the highest mode value of the second mode.

Figure 12 compares the control forces exerted by the LTMD and TMD. The constraint forces at node 10 of the LTMD corresponding to two cases are shown in Figure 12(a). It is shown that the constraint forces in case 1 are a little higher than those in case 2. And, it is observed that the control forces exhibited by the TMD are larger than the constraint forces by the LTMD. Thus, it is found that the displacement responses can be more explicitly controlled by distributing the control effect of the TMD system into two nodes of the LTMD.

It can be expected from the above two applications that the LTMD can be more effective in controlling the dynamic responses of a low-rise building structure with a few DOFs than those of a high-rise building structure with many DOFs.

4. Conclusions

This study illustrates the effectiveness of the vibration control by the LTMD. The LTMD controls the dynamic responses combining the TMD parameters and the constraint condition. Though the optimum parameter values of the LTMD cannot be explicitly established, they can be estimated by numerical experiments. The numerical applications exhibit that the LTMD leads to remarkable

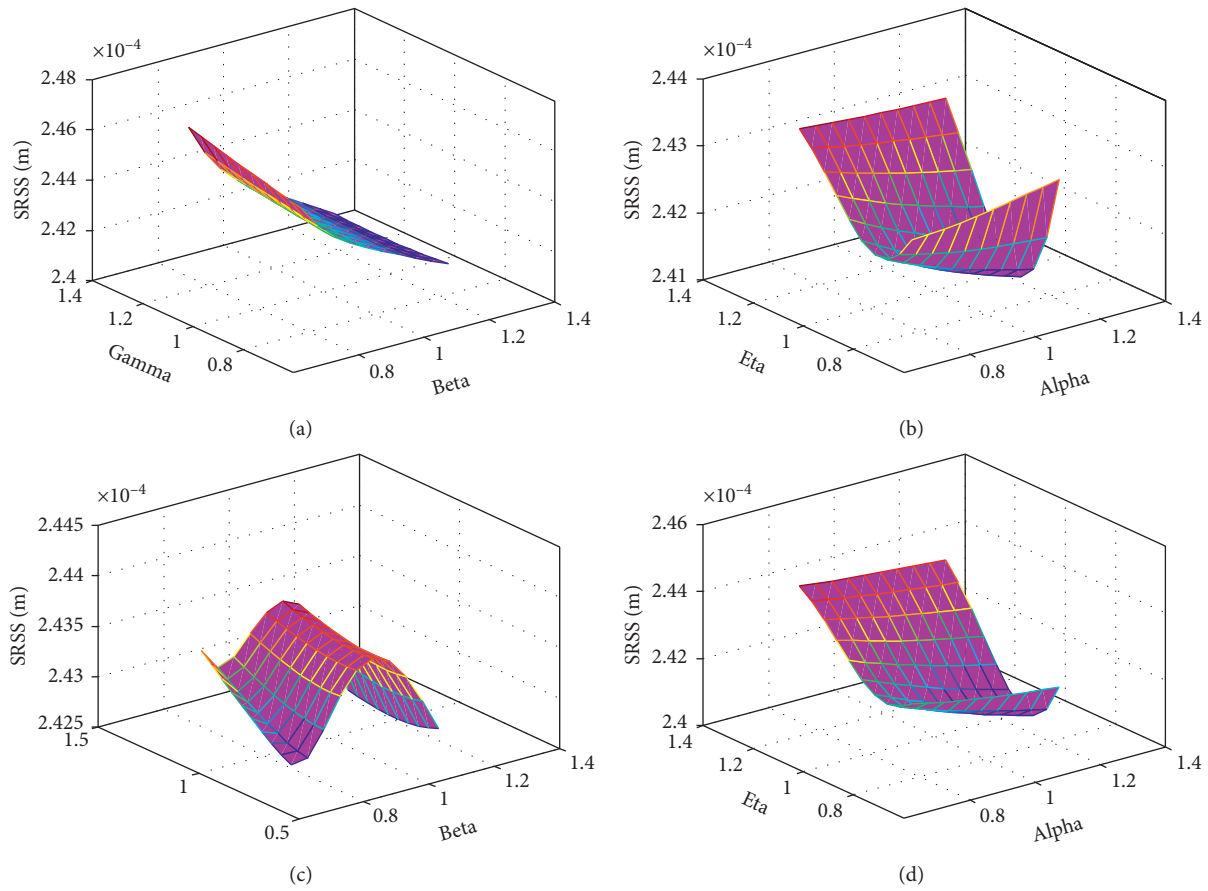

Figure 9: Comparison of numerical results depending on installation location ($\mu = 0.03$) of nodes 10 and 15 and 10 and 13. (a) SRSS of case 1 when $\alpha = 1.414$, $\beta = 1.15$, $\gamma = 0.95$, and $\eta = 1.0$; (b) SRSS of case 2 when $\alpha = 1.15$, $\beta = 1.15$, $\gamma = 0.95$, and $\eta = 0.85$; (c) SRSS of case 1 when $\alpha = 1.122$, $\beta = 1.15$, $\gamma = 0.9$, and $\eta = 1.0$; (d) SRSS of case 2 when $\alpha = 1.15$, $\beta = 1.15$, $\gamma = 0.9$, and $\eta = 0.8$.

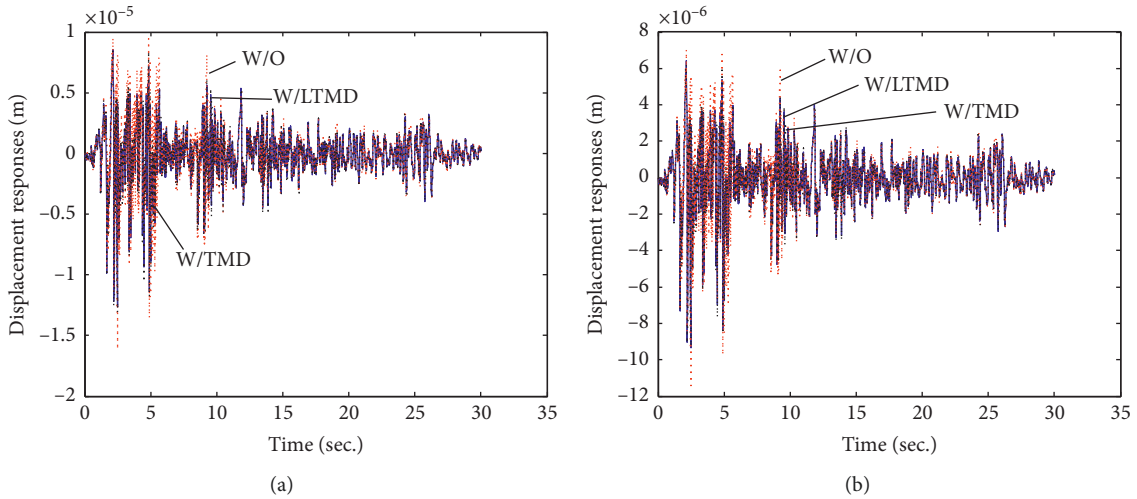

Figure 10: Continued.

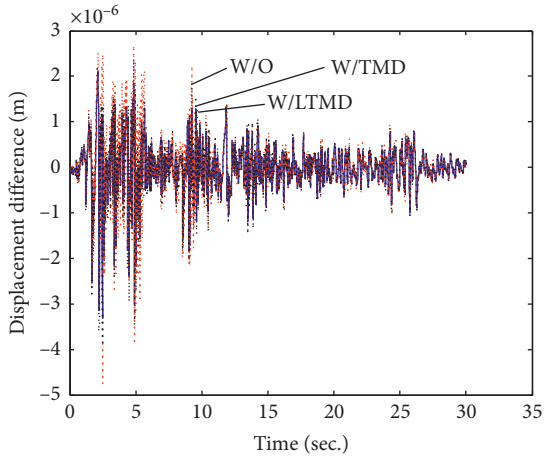

(c)

Figure 10: Displacement responses at nodes 10 and 15 ($\mu = 0.03$) of case 1 using $\alpha = 1.15$, $\beta = 1.15$, $\gamma = 0.95$, and $\eta = 0.85$. (a) Displacement responses at node 10; (b) displacement responses at node 15; (c) displacement difference between nodes 10 and 15.

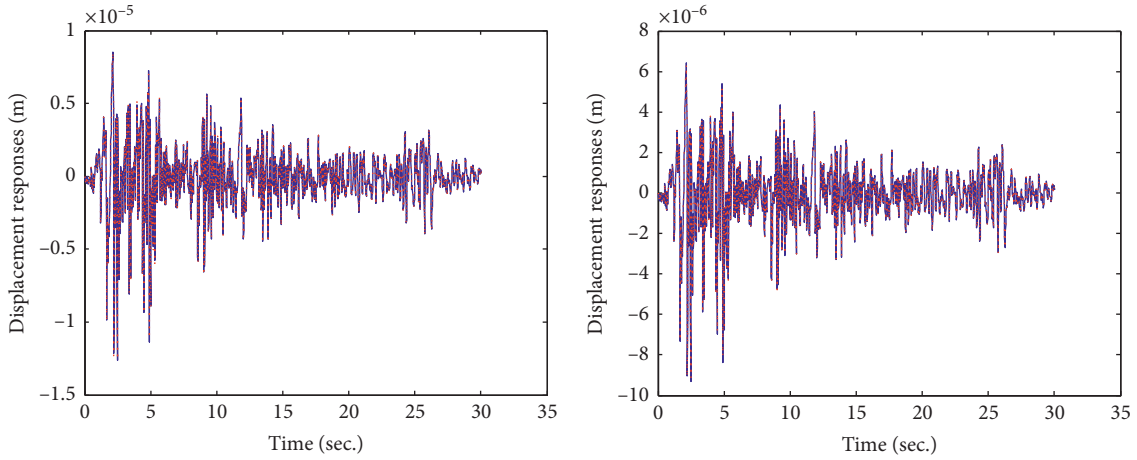

(a) (b)

Figure 11: Comparison of displacement responses of cases 1 and 2. (a) Displacement responses at node 10; (b) displacement responses at node 15.

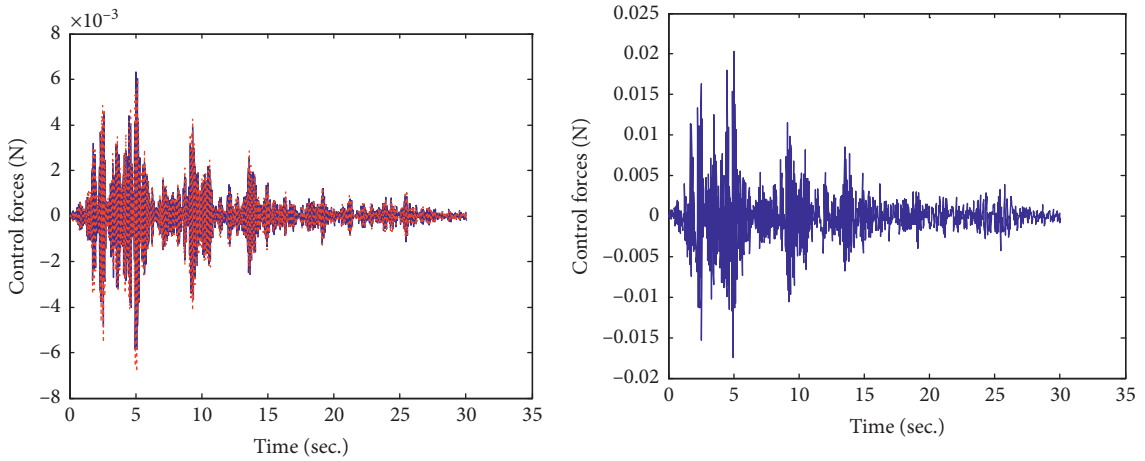

(a) (b)

Figure 12: Comparison of control forces by the TMD and LTMD at node 10. (a) Constraint forces exhibited by the LTMD; (b) control forces exhibited by the TMD.

displacement reduction. And, the LTMD is more effective control system than the TMD because the LTMD controls the displacements between adjacent floors. The control effect by the LTMD is more sensitive to the length ratio of the lever and the stiffness ratio at both ends of the lever than the other parameters. The LTMD is a little more effective when it is installed at the location of the highest mode value of the second mode. It is found that the displacement responses can be more explicitly controlled by distributing the control effect of the TMD system into two nodes of the LTMD.

Data Availability

The data used to support the findings of this study are included within the article.

Conflicts of Interest

The authors declare that they have no conflicts of interest.

Acknowledgments

This study was supported by the 2018 Research Grant (PoINT) from Kangwon National University.

References

[1] J. Ormondroyd and J. P. Den Hartog, "The theory of the vibration absorber," *Transactions of the American Society of Mechanical Engineers*, vol. 49, pp. A9–A22, 1928.

[2] H.-C. Tsai and G.-C. Lin, "Optimum tuned-mass dampers for minimizing steady-state response of support-excited and damped systems," *Earthquake Engineering & Structural Dynamics*, vol. 22, no. 11, pp. 957–973, 1993.

[3] I. Abdulsalam, M. Al-Janabi, and M. G. Al-Taweel, "Optimum design of tuned mass damper systems for seismic structures," *Seismic Control Systems*, vol. 59, pp. 175–184, 2012.

[4] J. P. Den Hartog, *Dynamic Vibration Absorbers*, Mechanical Engineering Publications University of California, Oakland, CA, USA, 1979.

[5] I. M. Abubakar and B. J. M. Farid, "Generalized Den Hartog tuned mass damper system for control of vibrations in structures," *WIT Transactions on The Built Environment*, vol. 104, pp. 185–193, 2009.

[6] M. R. Okhovat, M. Rahimian, and A. K. Ghorbani-Tanha, "Tuned mass damper for seismic response reduction of Tehran Tower," in *Proceedings of the 4th International Conference on Earthquake Engineering*, Taipei, Taiwan, 2006.

[7] M. M. Murudi and S. M. Mane, "Seismic effectiveness of tuned mass damper for differenct ground motion parameters," in *Proceedings of the 13th World Conference on Earthquake Engineering*, Vancouver, BC, Canada, August 2004.

[8] G. B. Warburton and E. O. Ayorinde, "Optimum absorber parameters for simple systems," *Earthquake Engineering & Structural Dynamics*, vol. 8, no. 3, pp. 197–217, 1980.

[9] A. A. Farghaly and M. S. Ahmed, "Optimum design of TMD system for tall buildings," *ISRN Civil Engineering*, vol. 2012, Article ID 716469, 13 pages, 2012.

[10] S. M. Nigdeli and G. Bekdas, "Performance comparison of location of optimum TMD on seismic structures," *International Journal of Theoretical and Applied Mechanics*, vol. 3, pp. 99–106, 2018.

[11] S. V. Bakre and R. S. Jangid, "Optimum parameters of tuned mass damper for damped main system," *Structural Control and Health Monitoring*, vol. 14, no. 3, pp. 448–470, 2007.

[12] N. D. Stoica, "Using modern methods of retrofitting existing seismic vulnerable buildings," in *Proceedings of the 13th SGEM GeoConference on Science and Technologies in Geology Exploration and Mining*, Sofia, Bulgaria, 2013.

[13] A. Brendike and Y. Petryna, "Seismic retrofitting of reinforced concrete frame structures by tuned mass dampers," in *Proceedings of the 8th International Conference on Structural Dynamics EURODYN*, Leuven, Belgium, July 2011.

[14] T. Suzuki, I. Kaneki, and T. Katsukawa, "Application of the powerful TMD as a measure for seismic retrofit of old bridges," in *Proceedings of the 12th World Conference on Earthquake Engineering*, Auckland, New Zeland, February 2000.

[15] P. Nawrotzki, T. Popp, and D. Siepe, "Seismic retrofitting of structures with tuned-mass systems," in *Proceedings of the 15th World Conference on Earthquake Engineering*, Lisbon, Portugal, September 2012.

[16] G. B. Warburton, "Optimum absorber parameters for various combinations of response and excitation parameters," *Earthquake Engineering & Structural Dynamics*, vol. 10, no. 3, pp. 381–401, 1982.

[17] F. Sadek, B. Mohraz, A. W. Taylor, and R. M. Chung, "A method of estimating the parameters of tuned mass dampers for seismic applications," *Earthquake Engineering & Structural Dynamics*, vol. 26, no. 6, pp. 617–635, 1997.

[18] F. E Udwadia and R. E. Kalaba, "A new perspective on constrained motion," *Proceedings of the Royal Society A: Mathematical, Physical and Engineering Sciences*, vol. 439, no. 1906, pp. 407–410, 1992.